Protein Immobilization Capabilities of Sucrose and Trehalose Glasses: The Effect of Protein/Sugar Concentration Unraveled by High-Field EPR

Protein Immobilization Capabilities of Sucrose and Trehalose Glasses: The Effect of Protein/Sugar Concentration Unraveled by High-field EPR

Marco Malferrari[1], Anton Savitsky[2,*], Wolfgang Lubitz[2], Klaus Möbius[2,3,*], Giovanni Venturoli[1,4,*]

[1] Laboratorio di Biochimica e Biofisica Molecolare, Dipartimento di Farmacia e Biotecnologie, FaBiT, Università di Bologna, I-40126 Bologna, Italy.

[2] Max-Planck-Institut für Chemische Energiekonversion, D-45470 Mülheim (Ruhr), Germany

[3] Fachbereich Physik, Freie Universität Berlin, D-14195 Berlin, Germany

[4] Consorzio Nazionale Interuniversitario per le Scienze Fisiche della Materia (CNISM), c/o Dipartimento di Fisica e Astronomia (DIFA), I-40126 Bologna, Italy.

AUTHOR INFORMATION

Corresponding Authors:

K. Möbius, e-mail: moebius@physik.fu-berlin.de

A. Savitsky, e-mail: anton.savitsky@cec.mpg.de

G. Venturoli, e-mail: giovanni.venturoli@unibo.it

ABSTRACT

Disaccharide glasses are increasingly used to immobilize proteins at room temperature for structural/functional studies and long-term preservation. To unravel the molecular basis of protein immobilization, we studied the effect of sugar/protein concentration ratios in trehalose or sucrose matrices, in which the bacterial photosynthetic reaction center (RC) was embedded as a model protein. The structural, dynamical, and H-bonding characteristics of the sugar/protein systems were probed by high-field W-band EPR of a matrix-dissolved nitroxide radical. We discovered that RC immobilization and thermal stabilization, being independent of the protein concentration in trehalose, occur in sucrose only at sufficiently low sugar/protein ratios. EPR reveals that only under such conditions sucrose forms a microscopically homogeneous matrix that immobilizes, via H-bonds, the nitroxide probe. We conclude that the protein immobilization capability depends critically on the propensity of the glass-forming sugar to create intermolecular H-bond networks, thus establishing a long-range, homogeneous connectivity within the matrix.

TOC GRAPHICS

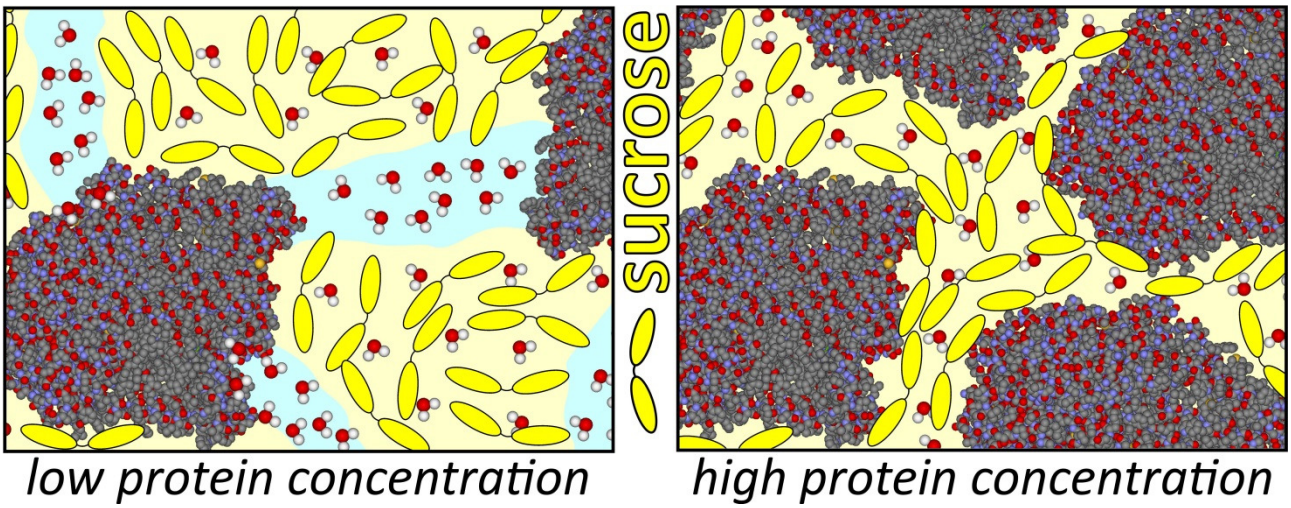

KEYWORDS Disaccharide glasses, trehalose, sucrose, protein stabilization, bacterial reaction center, high-field EPR.

The intriguing stability properties of proteins incorporated in solid sugar matrices are a subject of active research (for a comprehensive review, see [1]). Glassy disaccharide matrices such as sucrose and trehalose exhibit an outstanding capability to immobilize embedded biomolecules already at room temperature (RT). In basic research, such disaccharide systems greatly facilitate function/dynamics studies, because the conformational dynamics of the incorporated protein can be tuned at physiological temperatures by controlling the hydration level of the matrix. Under dried conditions, a retardation of protein dynamics, which mimics the effects of cryogenic temperatures, can be attained. [2-6] Disaccharide glasses have been employed recently as RT immobilizers of proteins [7] and nucleic acids [8] also for structural studies, based on pulsed dipolar EPR. In biotechnological applications trehalose-sugar glasses have received a wide interest to stabilize labile biostructures, optimizing their long-term storage at RT in the solid state. [9-10] These multifarious uses have been inspired by naturally occurring organisms that exploit the bioprotective action of trehalose, sucrose and other disaccharide glasses to withstand long periods of extreme draught and high temperatures by preserving the integrity of their cellular structures, while reversibly arresting their metabolism (*anhydrobiosis*). [11]

Despite the large efforts devoted to understand biopreservation phenomena during the last decades, the underlying molecular mechanisms remain unclear in many respects, and several, often complementary, hypotheses have been proposed. [12-17] In the case of proteins a large body of *in vitro* and *in silico* studies shows that the conformational immobilization reflects a tight protein-matrix dynamical coupling, promoted by a network of hydrogen bonds that involves exposed protein groups, sugar and residual water molecules [1, 18] (see also the recent differential-scanning-calorimetry (DSC) and viscometry work on the role of trehalose for the stabilization of proteins[19]). The structural organization of the protein-disaccharide matrices is therefore expected to play a critical role in bioprotection.

To clarify the protein-matrix interactions, glasses formed by trehalose and by the homologous disaccharide sucrose (Figure 1) have been compared in molecular detail, revealing a weaker *in vitro*

inhibition of conformational dynamics in sucrose, [16, 20] although *in vivo* large amounts of this disaccharide are expressed by anhydrobiotic higher plants. [21] In a previous study, [22] aimed at elucidating the physical basis of the superior bioprotective efficacy of *in vitro* trehalose, we probed the structural and dynamical characteristics of binary trehalose-water and sucrose-water matrices by means of high-field W-band EPR, using a nitroxide radical as electron-spin probe embedded in the glasses. In line with the tighter protein-matrix coupling concept in trehalose glasses, the EPR spectra of the nitroxide show that in dried trehalose systems the guest molecules are homogeneously integrated into a hydrogen-bond network of water-trehalose, which strongly restricts their mobility. In contrast, dehydrated sucrose forms a highly heterogeneous matrix, which includes polycrystalline clusters and different amorphous domains, where residual water and guest molecules accumulate, retaining a considerable mobility.

In the present letter we address, at the molecular level, the problem of the peculiar trehalose protein stabilization by comparing the protein immobilization capabilities of sucrose and trehalose in amorphous ternary sugar-water-protein systems. To this end we probe in parallel their structural and dynamical organization via W-band EPR of a nitroxide radical dissolved in the respective matrices. We demonstrate that the protein concentration within the matrices governs the matrix/protein coupling in sucrose, but not in trehalose. This is because only in the sucrose system the structural and dynamical properties are affected by the sugar/protein molar ratio.

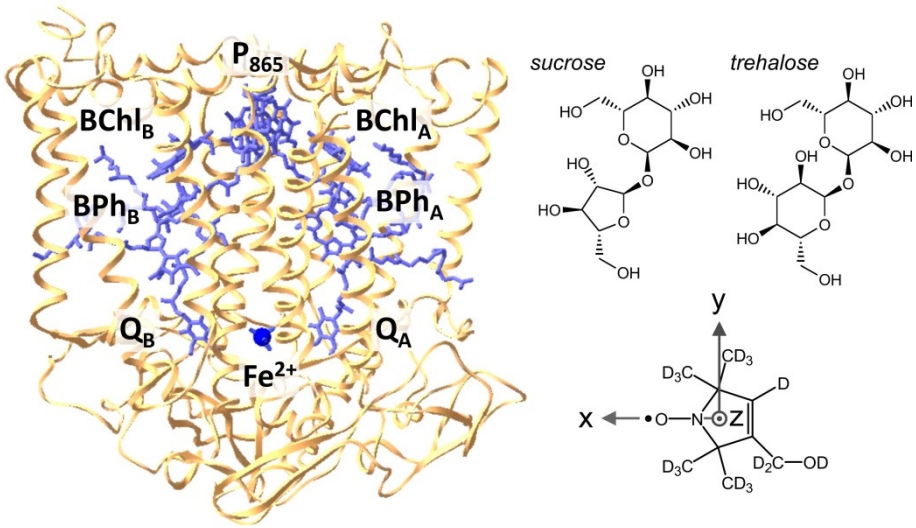

Figure 1. Structure of the RC from *Rb. sphaeroides* R-26, of the perdeuterated pyrroline type nitroxide radical, and of the disaccharides sucrose and trehalose used as glass formers. RC cofactor abbreviations: P_{865}, bacteriochlorophyll *a* dimer; BChl, bacteriochlorophyll *a* monomer; BPh, bacteriopheophytin *a*; Q, ubiquinone-10; Fe^{2+}, non-heme iron. A and B indices refer to the two protein-cofactor branches related by a pseudo-C_2 symmetry.

As a model guest protein we used the bacterial photosynthetic reaction center (RC) from *Rhodobacter* (*Rb.*) *sphaeroides* R-26 (Figure 1). Within this pigment-protein complex, [23] following photoexcitation, an electron is delivered from the primary electron donor P_{865}, a bacteriochlorophyll dimer, to the primary quinone acceptor Q_A, generating the primary charge-separated state $P_{865}^{\bullet+}Q_A^{\bullet-}$. When electron transfer to the secondary quinone acceptor Q_B is prevented, the electron on Q_A recombines with the hole on P. The kinetics of $P_{865}^{\bullet+}Q_A^{\bullet-}$ recombination after a short (nanosecond) laser pulse (Figure 2) provides an endogenous probe of the RC internal dynamics. In RT solutions, following charge separation, the RC relaxes from a *dark-adapted* to a *light-adapted* conformation, which stabilizes energetically the $P_{865}^{\bullet+}Q_A^{\bullet-}$ state (lifetime ≈100 ms). When such a relaxation is blocked (by freezing the RC in the dark [24] or by incorporating it into RT trehalose glasses [4]), the recombination kinetics, as observed for RCs in solution, accelerate ($P_{865}^{\bullet+}Q_A^{\bullet-}$ lifetime ≈20 ms) and become distributed, reflecting the freezing of the protein yielding a large ensemble of conformational substates. Thus, we use a continuous distribution *p(k)* of rate constants to describe the survival probability *N(t)* of the $P_{865}^{\bullet+}Q_A^{\bullet-}$ state after photoexcitation by a laser pulse [4]

$$N(t) = \int_0^\infty p(k)\, exp(-kt)dk \; = (1+\lambda t)^{-n} \qquad (1)$$

with λ and *n* as adjustable parameters. [25] Fitting *N(t)* to a power law implies that *p(k)* is a Gamma distribution, $p(k) = [k^{n-1}exp(-k/\lambda)]/[\lambda^n \Gamma(n)]$, where $\Gamma(n)$ is the Gamma function. The average rate constant, $\langle k \rangle$, and the variance σ^2 of *p(k)* are given by [26] $\langle k \rangle = n\lambda$ and $\sigma^2 = n\lambda^2$.

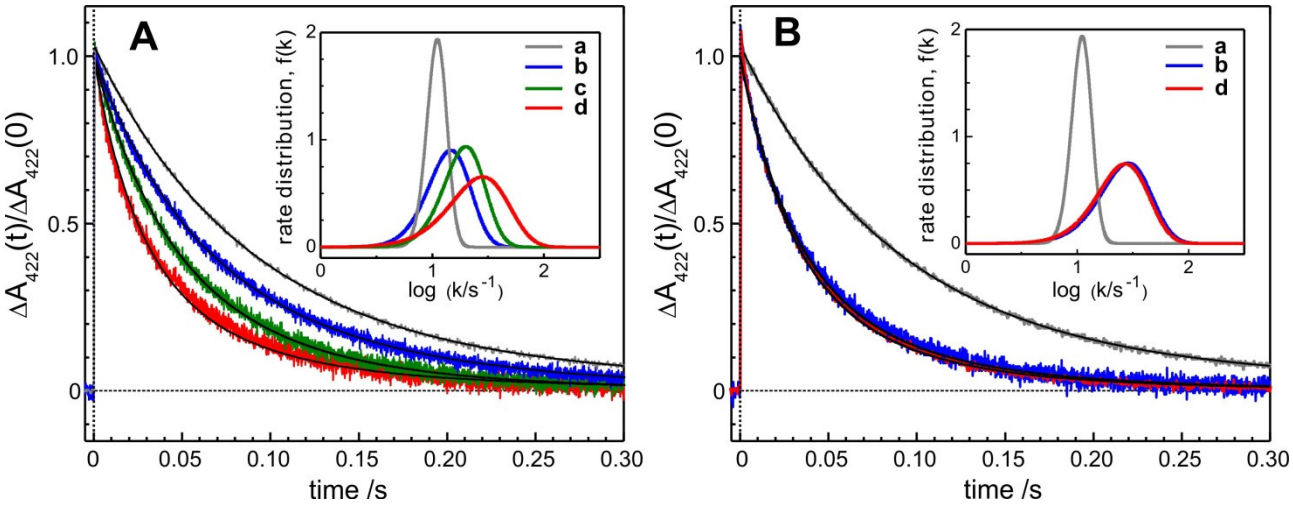

Figure 2. The effect of the (sugar/protein) molar ratio *m* on the kinetics of $P_{865}^{\bullet+}Q_A^{\bullet-}$ recombination in RC-sucrose (**A**) and RC-trehalose glasses (**B**) at the same relative humidity, *r* = 11%. Charge recombination after the laser pulse (at *t* = 0) has been monitored by optical absorption spectroscopy. Traces *b* (blue), *c* (green), and *d* (red) refer to *m* values equal to 10^4, $5{\cdot}10^3$, and 10^3, respectively. Kinetics in a liquid RC suspension, trace *a* (grey), are shown for comparison. Black curves are the best fit to Eq.1. The insets show the corresponding rate-distribution functions *f(k)* on a logarithmic scale [*p(k) dk = f(k) d log(k)*]. Values of average rate constants <*k*>, distribution widths σ, and residual water contents of the matrices are reported in Table S2 of Supporting Information.

In essence, <*k*> and σ report on the conformational dynamics of the RC: An increase in <*k*> and/or in σ mirrors a retardation of the RC relaxation from the *dark-* to the *light-adapted* conformation and/or of the interconversion between conformational substates, respectively. [5] Based on this rationale, Figure 2 compares the kinetics of $P_{865}^{\bullet+}Q_A^{\bullet-}$ after a laser flash in sucrose-RC (panel A) and trehalose-RC glasses (panel B) at sugar/RC molar ratios *m* from 10^3 to 10^4. At low protein concentration, *m* = 10^4 (blue traces), dehydration of sucrose-RC glasses results in a modest acceleration of the kinetics and limited distribution broadening, as compared to trehalose-RC glasses. However, the decrease of *m* to $5{\cdot}10^3$ (green traces) and to 10^3 (red traces) markedly accelerates $P_{865}^{\bullet+}Q_A^{\bullet-}$ recombination, and broadens the rate constant distribution (Figure 2A). In contrast, in the trehalose-RC glasses, a variation of the sugar/RC molar ratio over the same range has essentially no effect on the kinetics (Figure 2B). We infer that, at variance with trehalose, the

efficacy of dried sucrose matrices in inhibiting the RC conformational dynamics strongly depends upon the sugar/RC molar ratio: Conformational immobilization of the RC on the time scale of $P_{865}^{\bullet+}Q_A^{\bullet-}$ recombination is only achieved at the highest protein concentration. The same conclusion has been reached by using transient W-band EPR detection of P^+ to probe the kinetics of $P_{865}^{\bullet+}Q_A^{\bullet-}$ recombination (Supporting Information (SI), Figure S1).

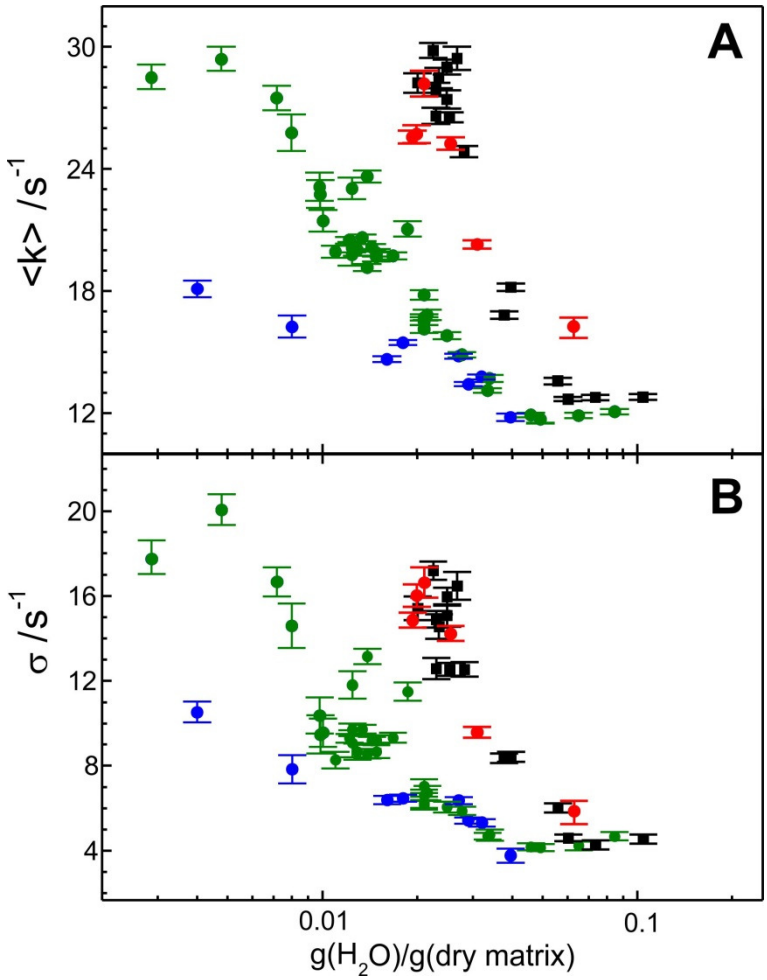

Figure 3. Dependence of $P_{865}^{\bullet+}Q_A^{\bullet-}$ recombination kinetics upon the residual water content in sucrose-RC matrices with different sugar/protein molar ratios: $m = 10^3$ (red); $m = 5 \cdot 10^3$ (green); $m = 10^4$ (blue). average rate constant, $\langle k \rangle$, (panel A) and distribution width, σ, (panel B) values have been obtained as illustrated in Figure 2. The dependence observed in a trehalose-RC glass, at $m = 5 \cdot 10^{3,}$ is also shown in black for comparison. The vertical bars represent confidence intervals within 2 standard deviations.

Figure 3 presents a systematic study of this effect when varying the residual water content in the sucrose matrices. The increase of $\langle k \rangle$ with dehydration (panel A) reflects the retardation of the

RC relaxation from the *dark-* to the *light-adapted* conformation, paralleled by hindering of thermal fluctuations between conformational substates (increase of σ in panel B). Figure 3 shows that the response to dehydration is dramatically modulated by the sugar/protein molar ratio: Under the driest conditions of the sucrose-RC matrix internal motions are barely inhibited at $m = 10^4$, but blocked at $m = 10^3$, as observed in trehalose-RC matrices. At the intermediate molar ratio ($m = 5 \cdot 10^3$) the sucrose matrix reduces the RC dynamics comparably to that of the trehalose glass, but only at considerably lower hydration levels.

In view of the above results we expect that the sugar/RC molar ratio also strongly affects the thermal stability of RCs embedded in sucrose matrices. This was confirmed by comparing the denaturation kinetics at 44 °C of RCs embedded in dehydrated sucrose matrices characterized by $m = 10^4$ and 10^3: At a high sugar/RC molar ratio ($m = 10^4$) the RC loses its native structure on the time scale of hours (Figure S2A and Figure S3); in contrast, at $m = 10^3$, essentially no denaturation occurs even after exposure to 44 °C for approximately one week (Figure S2B). By and large, the ability of dried sucrose matrices to hinder both small-scale, fast conformational relaxations of the RC (coupled to $P_{865}^{\bullet+}Q_A^{\bullet-}$ recombination) and large-scale, slow structural rearrangements (associated with RC denaturation) depends critically upon *m*.

We investigated the molecular basis for this striking sensitivity to the sugar/protein ratio by W-band EPR spectroscopy of a nitroxide radical (Figure 1) dispersed in the ternary sucrose-RC-water amorphous systems. [22, 27] Preliminarily acquired EPR spectra of the nitroxide in water solutions at RT both in the presence or absence of the RC are diagnostic of a freely rotating, unbound probe (SI, Figure S4), suggesting no preferential interaction of the spin probe with the RC-detergent complex.

Figure 4A shows W-band cw EPR spectra of nitroxide radicals embedded into sucrose-RC matrices at RT with sugar/RC ratios of 10^3, $5 \cdot 10^3$ and 10^4, dehydrated to a relative humidity r = 11%. For comparison, the spectrum recorded in a trehalose-RC glass, with $m = 10^4$, is also

presented. The latter is characterized by the typical lineshape of a homogeneous distribution of immobilized nitroxide radicals. Three distinct B_0 magnetic field regions, corresponding to the principal values of the g-tensor (g_{xx}, g_{yy} and g_{zz}) are clearly resolved and, in the g_{yy} and g_{zz} regions, the nitrogen ^{14}N hyperfine splitting into line triplets (I(^{14}N) = 1, hyperfine tensor (A_{xx}, A_{yy}, A_{zz})), is observed.

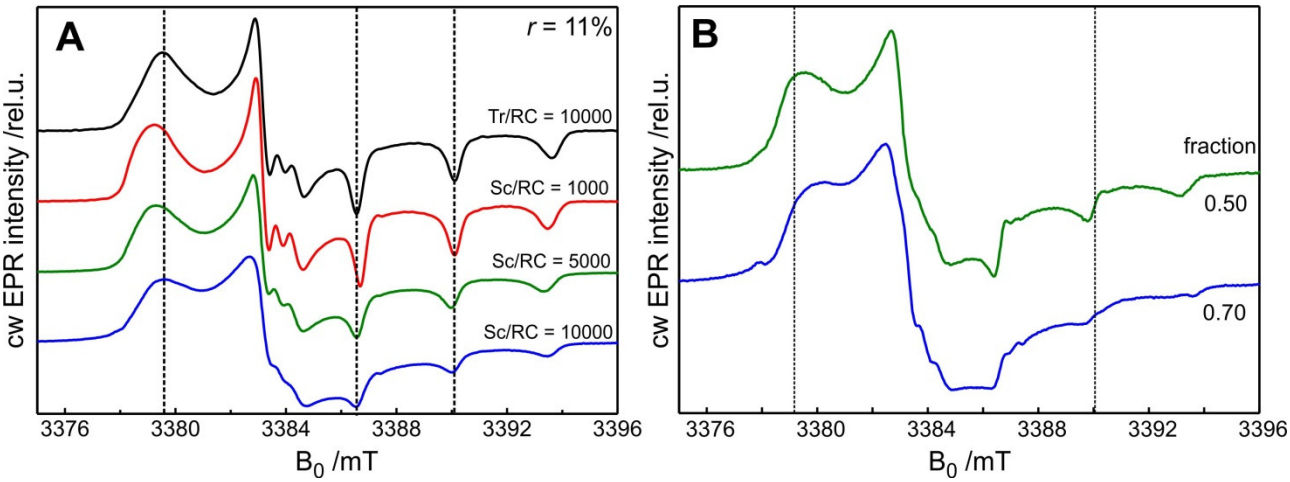

Figure 4. **(A)** W-band cw EPR spectra of the nitroxide radical in trehalose (Tr)-RC and sucrose (Sc)-RC matrices characterized by different sugar/RC molar ratios, equilibrated at r = 11% and acquired at 293 K. **(B)** Deconvolution results of the W-band cw EPR spectrum of the nitroxide radical in sucrose/RC matrix at different sugar/RC molar ratios. The spectra were obtained by substraction of the properly normalized spectrum in Sc/RC = 1000 matrix from the spectra with higher molar ratios. The relative integral weights of the deconvoluted EPR spectra of high mobility nitroxide fractions are given at the respective spectra.

For the trehalose-RC glass, a satisfactory simulation of the spectrum can be obtained using a single set of magnetic interaction parameters (g_{ii} and A_{ii}), demonstrating that the nitroxide radical is exposed to a homogeneous microenvironment. Multi-parameter best fitting, obtained through numerical solution of the spin Hamiltonian, yields g- and A-tensor principal values of g = [2.0083; 2.0059; 2.0022] and A = [0.56; 0.57; 3.69] mT (Figure S6). The spectrum closely reproduces the one measured in a trehalose-water binary matrix at the same r, (g = [2.0082; 2.0060; 2.0024] and A = [0.58; 0.58; 3.75] mT) [22]. This strongly suggests that the presence of the embedded RC does not affect significantly the structural and dynamical features of dry trehalose matrices.

The spectra in the sucrose-RC matrices disclose quite a different scenario. At a sugar/RC molar ratio of $m = 10^3$ the spectrum is similar to that in the trehalose-RC glass, indicating that the nitroxides are comparably immobilized and experience a similar homogeneous microenvironment. However, the EPR spectrum reveals a low-field shift of the g_{xx} spectral component as well as a lower A_{zz} value in sucrose as compared to trehalose (Figure S5), which are indicative of the different hydrogen-bonding situations in both matrices (see ref. [28-29] and references therein). Multi-parameter best fitting to the spectrum in sucrose yields g = [2.0086; 2.0059; 2.0022] and A = [0.55; 0.55; 3.53] mT (Figure S6). When m is increased to $5 \cdot 10^3$ and to 10^4, the spectra undergo changes which mirror a progressive loss of homogeneity and the presence of radical subpopulations characterized by an increased mobility. Figure 4B shows the EPR spectra of these mobile fractions obtained by the subtraction of a properly normalized EPR spectrum, recorded for a sugar/RC molar ratio of $m = 10^3$, from the spectra for higher molar ratios. Increasing the molar ratio from 10^3 to $5 \cdot 10^3$ results in the appearance of a nitroxide fraction with increased mobility with a relative weight of 0.5. The mobility and relative weight (0.7) further increase for the sample with a sucrose/RC molar ratio of $m = 10^4$.

The molecular information emerging from these results is fully consistent with the effects of the sucrose/RC molar ratio on the RC dynamics, and on the thermal stability of the RC, as described above. The EPR spectral analysis, in fact, indicates that at high protein concentration ($m = 10^3$), the hosted molecules are strongly immobilized within an essentially homogeneous glass, mimicking what is observed in trehalose matrices, independent of the presence of the protein. When the protein is diluted by an increasing amount of sucrose (up to $m = 10^4$), the matrix loses its homogeneity, and an increasing subpopulation of the hosted molecules gains motional freedom, consistent with a weaker dynamical coupling between the amorphous matrix and embedded RC.

Notably, even at the lowest protein concentration ($m = 10^4$), the protein strongly affects the organization of the sucrose matrix: The EPR spectrum recorded in the RC-sucrose matrix at $m = 10^4$ is radically different from that observed in the binary system, which is dominated by a single

Lorentzian line. It reflects a matrix domain containing a large fraction (48%) of the nitroxide population, characterized by a very high local nitroxide concentration and a substantial amount of water caused by partial polycrystallization of sucrose. [22] The single dominating line disappears in the presence of the RC, indicating that a corresponding nanophase separation does not take place, although the ternary system remains heterogeneous.

As shown in Figure 3 (see also Table S1), under hydrated conditions both trehalose and sucrose matrices become ineffective in blocking the conformational dynamics of the embedded RC.[4, 16] In order to follow such a change of the sugar-protein dynamical coupling, and further characterize the effects of the protein on the structure and dynamics of the sugar matrices, W-band cw EPR spectra have been acquired in the same trehalose and sucrose glasses (previously equilibrated at $r = 11\%$, see Figure 4A), rehydrated at $r = 74\%$ (Figure 5A). For comparison, spectra recorded in the binary trehalose-water and sucrose-water systems, rehydrated at the same r value, are presented in Figure 5B. The nitroxide EPR spectrum in the rehydrated trehalose-RC matrix (Figure 5A) shows that softening of the matrix occurs due to increased water content. As result, slightly increased motional mobility of immobilized radicals is observed. Surprisingly, the matrix stays to a large extent homogeneous, in contrast to the pure trehalose matrix. In the absence of the protein, in fact, the trehalose matrix in its final stage of rehydration ($r = 74\%$) is characterized by the presence of three types of domains. [22] The first and second types, with high water content (low microscopic viscosity, very mobile nitroxides) and low water content (high microscopic viscosity, immobilized nitroxides), are directly probed by EPR (see Figure 5B). Thus, inclusion of the RC in the trehalose homogenizes the matrix composition and prohibits polycrystallization of trehalose. The sucrose-RC matrix composition strongly depends on the RC/sugar molar ratio. For the highest protein concentration ($m = 10^3$) the EPR spectrum reveals two fractions of the nitroxides. The larger fraction contains the radicals with higher mobility as compared to those imbedded in the trehalose-RC matrix. Decrease of the protein concentration leads to an increase of radical mobility in this fraction. Whereas the EPR spectrum recorded for the sucrose-RC matrix with $m = 5 \cdot 10^3$ roughly

agrees with that observed in pure sucrose (see Figure 5B). Thus, at this RC concentration, the RC-sucrose matrix resembles the behavior of pure sucrose. One would expect that the nitroxide EPR spectrum in the latter matrix (binary sucrose-water system) is more similar to that measured in the RC-sucrose matrix at the lowest ($m = 10^4$), rather than at the intermediate ($m = 5 \cdot 10^3$) RC concentration, at variance with what is observed. A possible explanation for the larger probe mobility at $m = 10^4$ than in the pure sucrose matrix could be that at $r = 74\%$ the equilibrated matrix is more hydrated in the presence of the protein and/or that additional higher water concentration domains are appearing, presumably at the sugar-protein interface.

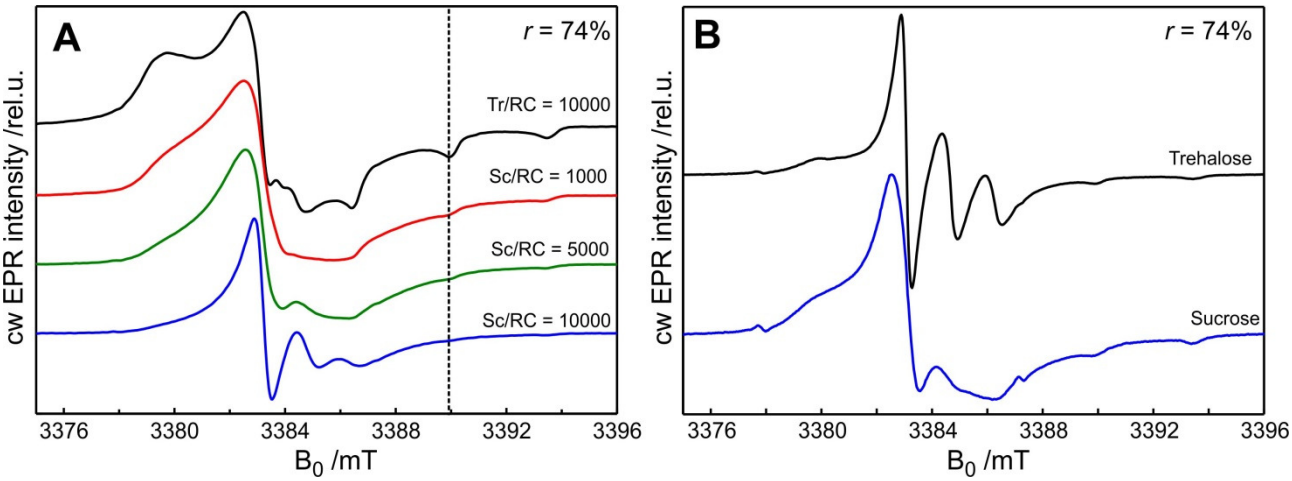

Figure 5. **(A)** W-band cw EPR spectra of the nitroxide radical in trehalose-RC and sucrose-RC matrices characterized by different sugar/RC molar ratios, equilibrated at $r = 11\%$ and subsequently rehydrated at $r = 74\%$. **(B)** W-band cw EPR spectra of the nitroxide radical in trehalose and sucrose matrices equilibrated at $r = 11\%$ and subsequently rehydrated at $r = 74\%$. All spectra are acquired at 293 K.

The results of the W-band EPR experiments allow us to conclude about the microscopic behavior of sucrose and trehalose matrices in the presence of the RC protein. Independent of the protein content, under dehydrated conditions trehalose forms a homogeneous matrix, which immobilizes the embedded nitroxide radical and RC protein. The dehydrated sucrose matrix behaves similarly only at sufficiently high concentrations of the RC protein. Decreasing the RC concentration within the sucrose matrix leads to the formation of at least two domains with lower and higher water content under both dehydrated and rehydrated conditions. For both matrices the

inclusion of RC prohibits the growing of sugar polycrystalline domains that are observed in dehydrated sucrose and rehydrated trehalose.[22]

Within the disaccharide (sucrose or trehalose) matrix, the mobility of the nitroxide (a very good H-bond acceptor) is expected to be mainly governed by its involvement in H-bonding with the local environment. The immobilization of homogeneously distributed nitroxide molecules appears therefore to reflect their inclusion in a sufficiently rigid and extended H-bond network. As mentioned above, the progressive homogenization and immobilization of the nitroxide probe population upon increasing the protein concentration in the dehydrated sucrose matrix (Figure 4) occurs in parallel with the retardation of the RC conformational dynamics (Figure 3) and the consequent prevention of thermal denaturation (see SI III). This strongly suggests that the inhibition of the RC dynamics is also due to the development of a long-range connectivity within the sugar-protein matrix, promoted by an extended H-bond network. This involves the sugar, the residual water molecules, and surface groups of the protein. Such a network would anchor the protein surface to the surrounding matrix, the rigidity of which depends on the hydration level (*anchorage hypothesis* [16]).

The above considerations lead us to propose that the main physical-chemical property, which determines the structural/dynamical organization of the disaccharide matrix, and consequently its protein immobilization capability, is the propensity of a particular disaccharide to form nonspecific inter-molecular hydrogen-bond networks. In spite of its structural similarity with trehalose, sucrose has a lower propensity to form inter-molecular H-bonds. In the crystalline form, sucrose forms two intra-molecular H-bonds between glucopyranosyl and fructofuranosyl,[30-31] while trehalose does not form any intra-molecular H-bond, both when dehydrated [32-33] and in the two anhydrous forms, Tre(α)[33] and Tre(β).[34] MD simulations in concentrated solutions indicate that the intra-molecular H-bonds found in the sucrose crystal structure are not broken in solution near the glass transition temperature. [35] Due to the formation of intra-molecular H-bonds sucrose has fewer sites disposable to form H-bonds with its surrounding. The intra-molecular H-bonds also make sucrose more rigid

than trehalose, as recently indicated by dielectric relaxation studies on the mobility of the glycosidic linkage below and above the glass transition temperature.[36] The comparison of EPR spectra of the nitroxide radical immobilized in RC-trehalose ($m = 10^4$) and RC-sucrose ($m = 10^3$) matrices (Figure S5 and S6) additionally supports the notion of a larger propensity of trehalose for inter-molecular H-bonding, as probed by the different g_{xx} and A_{zz} values in the two sugar matrices. [29] In the trehalose matrix, the nitroxide is more firmly incorporated in the H-bond network as compared to sucrose: In trehalose all radicals carry one H-bond, as revealed by the low-temperature EPR spectra (see Figure S7), while the spectrum in sucrose includes the contributions of both non- and one-H-bonded nitroxides.[29] In protein-sucrose matrices characterized by a low protein concentration, the rigidity of the sucrose matrix and its low propensity to H-bonding to nearby groups appear to be responsible for the structural and dynamical heterogeneity of the matrix: Besides sucrose polycrystalline clusters, and limited amorphous regions, it includes mostly domains in which the nitroxide probe and the RC protein retain a large mobility and conformational freedom, respectively. Increasing the RC concentration forces the formation of H-bonds between the protein surface (with its residual hydration layer) and the sucrose matrix, thus disturbing the development of sucrose clusters and favoring a progressively more extended H-bond network, which homogeneously incorporates the embedded RC, the nitroxide probe, residual water molecules and sucrose molecules. Such a perturbation of the H-bonding organization appears reasonable when considering the strong change in the protein/sucrose volume ratio upon varying the sucrose/RC ratio between $m = 10^4$ and $m = 10^3$. A simplified geometrical model[37] yields for the RC-detergent complex a total volume $V_P \approx 3.5 \cdot 10^5$ Å^3. When assuming an average molecular volume of the sugar[38], $V_S \approx 3.7 \cdot 10^2$ Å^3, a sugar/protein volume ratio in the matrix of about 10 and 1 can be estimated at low ($m = 10^4$) and high ($m = 10^3$) RC concentration, respectively. Interestingly, these values correspond, in a crude approximation (cubic lattice), to average distances between nearby proteins of about 85 and 15 Å, respectively. This estimate implies that at high protein concentration only a few layers of sucrose molecules can be accommodated in the matrix volume between nearby

proteins. It is not surprising therefore that the H-bonding pattern and the structure of the sucrose matrix are strongly re-arranged by the protein at such concentrations.

In conclusion, the effect of protein/sugar ratio is consistent with the notion that sugar-specific, long-range H-bond connectivity within the protein-water-saccharide amorphous matrix is the key property which controls the retardation of protein conformational dynamics and is responsible for thermal protein stabilization at low water content. The finding that the protein immobilization capability of a glassy sucrose matrix can be strongly modulated by varying the protein concentration provides new hints for optimizing the RT preservation of labile proteins and macromolecules in biopharmaceutical, solid state formulations. Additionally, the observed peculiar sensitivity of protein-sucrose matrices to the protein concentration can account for the *in vivo* protective role of sucrose in desiccation-tolerant plants, where sucrose (in place of trehalose) is the most abundant sugar accumulated when entering the state of anhydrobiosis.[39]

ASSOCIATED CONTENT

Supporting Information. Sample preparation details; W-band EPR measurements; Visible and near-infrared optical measurements; Comparison of $P_{865}^{\bullet+}Q_A^{\bullet-}$ recombination kinetics as probed by optical and W-band EPR spectroscopy; Kinetics of RC thermal denaturation; Additional experimental and simulated W-band EPR spectra of the nitroxide radical. This material is available free of charge via the Internet at http://pubs.acs.org (PDF).

ACKNOWLEDGMENT

This work was supported by the Max-Planck-Gesellschaft and the Cluster of Excellence RESOLV (EXC 1069) funded by the Deutsche Forschungsgemeinschaft (DFG). M.M. and G.V. acknowledge financial support from MIUR of Italy (RFO2014)

REFERENCES

1. Cordone, L.; Cottone, G.; Cupane, A.; Emanuele, A.; Giuffrida, S.; Levantino, M. Proteins in Saccharides Matrices and the Trehalose Peculiarity: Biochemical and Biophysical Properties. *Curr. Org. Chem.* **2015,** *19*, 1684-1706.
2. Hagen, S. J.; Hofrichter, J.; Eaton, W. A. Protein Reaction Kinetics in a Room-Temperature Glass. *Science* **1995,** *269*, 959-962.
3. Giuffrida, S.; Cottone, G.; Librizzi, F.; Cordone, L. Coupling between the Thermal Evolution of the Heme Pocket and the External Matrix Structure in Trehalose Coated Carboxymyoglobin. *J. Phys. Chem. B* **2003,** *107*, 13211-13217.
4. Palazzo, G.; Mallardi, A.; Hochkoeppler, A.; Cordone, L.; Venturoli, G. Electron Transfer Kinetics in Photosynthetic Reaction Centers Embedded in Trehalose Glasses: Trapping of Conformational Substates at Room Temperature. *Biophys. J.* **2002,** *82*, 558-568.
5. Malferrari, M.; Francia, F.; Venturoli, G. Retardation of Protein Dynamics by Trehalose in Dehydrated Systems of Photosynthetic Reaction Centers. Insights from Electron Transfer and Thermal Denaturation Kinetics. *J. Phys. Chem. B* **2015,** *119*, 13600-18.
6. Malferrari, M.; Savitsky, A.; Mamedov, M. D.; Milanovsky, G. E.; Lubitz, W.; Möbius, K.; Semenov, A. Y.; Venturoli, G. Trehalose Matrix Effects on Charge-Recombination Kinetics in Photosystem I of Oxygenic Photosynthesis at Different Dehydration Levels. *Biochim. Biophys. Acta - Bioenergetics* **2016,** *1857*, 1440-1454.
7. Meyer, V.; Swanson, M. A.; Clouston, L. J.; Boratynski, P. J.; Stein, R. A.; McHaourab, H. S.; Rajca, A.; Eaton, S. S.; Eaton, G. R. Room-Temperature Distance Measurements of Immobilized Spin-Labeled Protein by DEER/PELDOR. *Biophysical Journal* **2015,** *108* (5), 1213-1219.
8. Kuzhelev, A. A.; Shevelev, G. Y.; Krumkacheva, O. A.; Tormyshev, V. M.; Pyshnyi, D. V.; Fedin, M. V.; Bagryanskaya, E. G. Saccharides as Prospective Immobilizers of Nucleic Acids for Room-Temperature Structural EPR studies. *J. Phys. Chem. Lett.* **2016,** *7*, 2544-2548.
9. Ohtake, S.; Wang, Y. J. Trehalose: Current Use and Future Applications. *J. Pharm. Sci.* **2011,** *100*, 2020-2053.
10. Cicerone, M. T.; Pikal, M. J.; Qian, K. K. Stabilization of Proteins in Solid Form. *Advanced Drug Deliv. Rev.* **2015,** *93*, 14-24.
11. Crowe, L. M. Lessons from Nature: The role of Sugars in Anhydrobiosis. *Comp. Biochem. Physiol., Part A: Mol. Integr. Physiol.* **2002,** *131*, 505-513.
12. Carpenter, J. F.; Crowe, J. H. An Infrared Spectroscopic Study of the Interactions of Carbohydrates with Dried Proteins. *Biochemistry* **1989,** *28*, 3916-3922.
13. Belton, P. S.; Gil, A. M. IR and Raman-Spectrscopic Studies of the Interaction of Trehalose with Hen Egg-White Lysozyme. *Biopolymers* **1994,** *34*, 957-961.
14. Sampedro, J. G.; Uribe, S. Trehalose-Enzyme Interactions Result in Structure Stabilization and Activity Inhibition. The Role of Viscosity. *Mol. and Cell. Biochem.* **2004,** *256*, 319-327.
15. Cesaro, A. Carbohydrates - All Dried Up. *Nature Materials* **2006,** *5*, 593-594.
16. Francia, F.; Dezi, M.; Mallardi, A.; Palazzo, G.; Cordone, L.; Venturoli, G. Protein-Matrix Coupling/Uncoupling in "Dry" Systems of Photosynthetic Reaction Center Embedded in Trehalose/Sucrose: The Origin of Trehalose Peculiarity. *J. Am. Chem. Soc.* **2008,** *130*, 10240-10246.
17. Cicerone, M. T.; Douglas, J. F. Beta-Relaxation Governs Protein Stability in Sugar-Glass Matrices. *Soft Matter* **2012,** *8*, 2983-2991.
18. Cordone, L.; Cottone, G.; Giuffrida, S.; Palazzo, G.; Venturoli, G.; Viappiani, C. Internal Dynamics and Protein-Matrix Coupling in Trehalose-Coated Proteins. *Biochim. Biophys. Acta, Proteins Proteomics* **2005,** *1749*, 252-281.

19. Olsson, C.; Jansson, H.; Swenson, J. The Role of Trehalose for the Stabilization of Proteins. *J. Phys. Chem. B* **2016,** *120*, 4723-4731.
20. Giuffrida, S.; Cottone, G.; Cordone, L. Role of Solvent on Protein-Matrix Coupling in MbCO Embedded in Water-Saccharide Systems: A Fourier Transform Infrared Spectroscopy Study. *Biophys. J.* **2006,** *91*, 968-980.
21. Clegg, J. S. Cryptobiosis - a Peculiar State of Biological Organization. *Comp. Biochem. Physiol., B: Comp. Biochem.* **2001,** *128*, 613-624.
22. Malferrari, M.; Nalepa, A.; Venturoli, G.; Francia, F.; Lubitz, W.; Möbius, K.; Savitsky, A. Structural and Dynamical Characteristics of Trehalose and Sucrose Matrices at Different Hydration Levels as Probed by FTIR and High-Field EPR. *Phys. Chem. Chem. Phys.* **2014,** *16*, 9831-9848.
23. Feher, G.; Allen, J. P.; Okamura, M. Y.; Rees, D. C. Structure and Functioin of Bacterial Photosynthetic Reaction Centers. *Nature* **1989,** *339*, 111-116.
24. Kleinfeld, D.; Okamura, M. Y.; Feher, G. Electron-Transfer Kinetics in Photosynthetic Reaction Centers Cooled to Cryogenic Temperatures in the Charge-Separated State: Evidence for Light-Induced Structural Changes. *Biochemistry* **1984,** *23*, 5780-6.
25. Steinbach, P. J.; Chu, K.; Frauenfelder, H.; Johnson, J. B.; Lamb, D. C.; Nienhaus, G. U.; Sauke, T. B.; Young, R. D. Determination of Rate Distributions from Kinetic Experiments. *Biophys. J.* **1992,** *61*, 235-245.
26. Weisstein, E. W. Gamma Distribution. In *CRC Press, LLC,* http://mathworld.wolfram.com/GammaDistribution.html, 1999.
27. Roozen, M.; Hemminga, M. A. Molecular-Motion in Sucrose Water Mixtures in the Liquid and Glassy State as Studied by Spin Probe ESR. *J. Phys. Chem.* **1990,** *94*, 7326-7329.
28. Nalepa, A.; Möbius, K.; Lubitz, W.; Savitsky, A. High-Field ELDOR-Detected NMR Study of a Nitroxide Radical in Disordered Solids: Towards Characterization of Heterogeneity of Microenvironments in Spin-Labeled Systems. *J. Magn. Reson.* **2014,** *242*, 203-213.
29. Gast, P.; Herbonnet, R. T. L.; Klare, J.; Nalepa, A.; Rickert, C.; Stellinga, D.; Urban, L.; Möbius, K.; Savitsky, A.; Steinhoff, H. J.; Groenen, E. J. J. Hydrogen Bonding of Nitroxide Spin Labels in Membrane Proteins. *Phys. Chem. Chem. Phys.* **2014,** *16*, 15910-15916.
30. Jeffrey, G. A.; Takagi, S. Hydrogen-Bond Structure in Carbohydrate Crystals. *Acc. Chem. Res.* **1978,** *11*, 264-270.
31. Davies, D. B.; Christofides, J. C. Comparison of Intramolecular Hydrogen-Bonding Conformations of Sucrose-Containing Oligosaccharides in Solution and the Solid-State *Carbohydr. Res.* **1987,** *163*, 269-274.
32. Taga, T.; Senma, M.; Osaki, K. The Crystal and Molecular Structure of Trehalose Dihydrate. *Acta Cryst.* **1972,** *B28*, 3258-3263.
33. Nagase, H.; Ogawa, N.; Endo, T.; Shiro, M.; Ueda, H.; Sakurai, M. Crystal Structure of an Anhydrous Form of Trehalose: Structure of Water Channels of Trehalose Polymorphism. *J. Phys. Chem. B* **2008,** *112*, 9105-9111.
34. Jeffrey, G. A.; Nanni, R. The Crystal-Structure of Anhydrous α,α-Trehalose at -150°. *Carbohydr. Res.* **1985,** *137*, 21-30.
35. Ekdawi-Sever, N. C.; Conrad, P. B.; de Pablo, J. J. Molecular Simulation of Sucrose Solutions near the Glass Transition Temperature. *J. Phys. Chem. A* **2001,** *105*, 734-742.
36. Kaminski, K.; Kaminska, E.; Wlodarczyk, P.; Pawlus, S.; Kimla, D.; Kasprzycka, A.; Paluch, M.; Ziolo, J.; Szeja, W.; Ngai, K. L. Dielectric Studies on Mobility of the Glycosidic Linkage in Seven Disaccharides. *J.Phys. Chem. B* **2008,** *112*, 12816-12823.

37. Malferrari, M.; Francia, F.; Venturoli, G. Coupling between Electron Transfer and Protein-Solvent Dynamics: FTIR and Laser-Flash Spectroscopy Studies in Photosynthetic Reaction Center Films at Different Hydration Levels. *J. Phys. Chem. B* **2011,** *115*, 14732-14750.
38. Miller, D. P.; dePablo, J. J.; Corti, H. Thermophysical Properties of Trehalose and its Concentrated Aqueous Solutions. *Pharm. Res.* **1997,** *14*, 578-590.
39. Buitink, J.; Leprince, O. Glass Formation in Plant Anhydrobiotes: Survival in the Dry State. *Cryobiology* **2004,** *48*, 215-228.